Chapter 7

Lobatto Methods: A Study of Their Stability Characteristics

Mevlüde Yakit Ongun[1]

Ceren Uysal[2]

Abstract

This chapter presents an overview of Lobatto-type Runge-Kutta schemes derived from Gauss–Lobatto quadrature formulas.Since the collocation nodes include both endpoints of the integration interval, these methods possess several advantageous stability and geometric properties.. Their key feature is that both endpoints of each integration step serve as collocation nodes. Throughout the chapter, the formulation processes, Butcher tableaus, and stability properties of five primary sub-classes (Lobatto IIIA, IIIB, IIIC, IIIC*, and Generalized Lobatto, Lobatto IIID) are detailed.

Linear stability is first examined via A-stability and L-stability. In this context, it is demonstrated that the corresponding stability functions reduce to specific Padé approximations of the exponential function. For non-linear dynamics, B-stability is analyzed. Through this analysis, The analysis reveals that: among the variants considered, only Lobatto IIIC is algebraically stable, which implies B-stability.

Furthermore, geometric integration aspects, such as symplecticity, P-stability, and energy behavior on the imaginary axis, are explored. It is established that a highly effective symplectic integrator is generated when Lobatto IIIA and IIIB methods are coupled into a partitioned system. To consolidate these theoretical derivations, visual plots of the stability regions and a comprehensive comparison table are provided at the end of the chapter.

1 Prof. Dr., Suleyman Demirel University, mevludeyakit@sdu.edu.tr, ORCID ID: 0000-0003-2363-9395

2 Stud. MSc, Graduate School of Natural and Applied Sciences, Suleyman Demirel University, yl2530110008@ogr.sdu.edu.tr, ORCID ID:0009-0007-1640-4180

https://doi.org/10.58830/ozgur.pub1361.c5497

1. Introduction

The historical foundations of modern numerical integration methods can be traced to the work of Runge at the end of the nineteenth century. Subsequent contributions by Heun, Kutta and later researchers gradually led to the development of the Runge-Kutta framework used today. By extending Euler's method, Runge derived a two-stage, second-order scheme that laid the foundation for what would later become a major class of numerical integrators. In the early 20th century, researchers such as Heun and Kutta significantly advanced these ideas, leading to the systematic construction of higher-order methods. Building on Runge's framework, Kutta's contributions were particularly influential and ultimately gave rise to what are now known as Runge-Kutta (RK) methods. During this formative period, Heun proposed a three-stage, third-order method, while Kutta introduced both a four-stage fourth-order method and a six-stage fifth-order scheme. The pursuit of improved accuracy motivated the construction of methods with increasing stage numbers, and numerous researchers contributed to this development throughout the twentieth century, with notable contributions from Nyström (in 1925), Huta (in 1956), and Butcher (in 1964), who developed seven-stage sixth-order methods. By the late 1970s, Curtis and Hairer further extended explicit Runge-Kutta constructions to as many as 18 stages.

In parallel with the development of explicit schemes, the challenge of stiff differential equations motivated the study of implicit methods. Butcher's work in 1964 provided a unifying framework for implicit Runge–Kutta schemes, forming the basis of modern solvers for stiff systems. In the 1970s, he further introduced a graph-theoretic approach based on rooted trees, which enabled a systematic characterization of order conditions and greatly simplified the construction of higher-order methods. This perspective was refined by Burrage (1978a, 1978b), who investigated stability properties and developed criteria for predicting the performance of implicit schemes under varying dynamical regimes. Later, Hairer and Wanner (1993) extended these tree-based techniques to Hamiltonian systems, opening the way for geometric numerical integration (Griepentrog,1978;Brugnano et al., 2012; Brugnano et al.,2014)

More recent investigations have extended Runge-Kutta techniques to a wide variety of applications, including differential-algebraic systems and high-order collocation methods for complex engineering models. Brugnano and Magherini (2007) applied Runge–Kutta techniques to second-order differential-algebraic equations (DAEs), while Martín-Vaquero (2010) constructed 17th-order Radau IIA methods, highlighting their effectiveness in complex mechanical systems.

Within this context, Lobatto methods represent a natural progression from classical quadrature rules to structure-preserving integrators. Originally introduced by Lobatto in the context of quadrature formulas incorporating endpoint evaluations, these methods were not fully integrated into time-stepping frameworks until the systematic development of Runge–Kutta theory in the mid-20th century. A key milestone was the introduction of the Butcher tableau by Butcher (1964), which provided an algebraic structure for analyzing such methods. In the same period, Dahlquist (1978) introduced the concept of A-stability, which became fundamental in the analysis of stiff differential equations.

During the 1970s, attention shifted toward deeper stability properties. Ehle(1973) used Padé approximation techniques to define L-stability, offering a theoretical explanation for the stiffly accurate behavior of Lobatto IIIC methods. Subsequent work by Hairer, Lubich, and Roche (1989) established the relevance of these methods for differential-algebraic equations. This line of research culminated in the comprehensive treatment by Hairer and Wanner (1996), who formalized concepts such as B-stability and algebraic stability. More recently, Hairer, Lubich, and Wanner (2006) developed the framework of geometric numerical integration, showing that Lobatto IIIA and IIIB methods form a symplectic pair capable of preserving geometric properties such as energy behavior in Hamiltonian systems.

Overall, the evolution of Lobatto methods reflects their transformation from classical quadrature-based constructions into a powerful family of structure-preserving integrators. Today, they play a central role in the numerical treatment of stiff ODEs, differential-algebraic systems, and long-time simulations in areas such as celestial mechanics and Hamiltonian dynamics. (Boscarino,2007; Boscarino,2009)

2. Preliminaries

In many scientific and engineering applications, when the integrand is complex or known only at discrete points, analytical integration becomes impractical. Consequently, Numerical methods have therefore been developed to approximate integrals to within error tolerance (Burden & Faires, 2011).

The following standard quadrature rules provide background for the structural and stability analysis of Lobatto methods in later sections.

For equal subinterval $\Delta x = (b - a)/n$

Rectangle Rule:

$$I = \int_a^b f(x)dx \cong \Delta x \sum_{j=1}^{n} f(x_j)$$

Trapezoidal Rule:

$$I = \int_a^b f(x)dx \cong \frac{\Delta x}{2}\left[f(a) + f(b) + 2\sum_{j=1}^{n-1} f(a + j\Delta x)\right]$$

Simpson's 1/3 Rule:

$$I = \int_a^b f(x)dx \cong \frac{\Delta x}{3}\left[f(a) + f(b) + 4\sum_{\substack{j=1 \\ j=Tek}}^{n-1} f(a + j\Delta x) + 2\sum_{\substack{j=2 \\ j=Çift}}^{n-2} f(a + j\Delta x)\right]$$

Simpson's 3/8 Rule:

$$I = \int_a^b f(x)dx \cong \frac{3}{8}\Delta x\left[f(a) + f(b) + 3\sum_{\substack{j=1 \\ j=1,2,4,5,7,8,..}}^{n-1} f(a + j\Delta x) + 2\sum_{\substack{j=3 \\ j=3,6,9,..}}^{n-3} f(a + j\Delta x)\right]$$

Gauss–Legendre Quadrature:

$I = \int_{-1}^{1} f(x)dx \cong \sum_{i=1}^{n} f(x_i)\, w_i$

where the nodes x_i are the roots of the Legendre polynomials and w_i are the corresponding weight coefficients (Bulirsch et al, 2000;Süli, Mayers, 2003; Atkinson et.al, 2008,2009; Ranocha et al, 2020).

2.1 High-order Implicit Runge-Kutta(IRK) Methods and Butcher Tableau

Implicit Runge-Kutta schemes constitute one of the most powerful approaches for solving ordinary differential equations when stability requirements are dominant.. The coefficients defining an (s)-stage Runge-Kutta method are conveniently summarized by the Butcher tableau, which serves as a standard tool for the formulation and analysis of these methods. Different choices of nodes and coefficients give rise to various subclasses of implicit Runge-Kutta schemes. Among these subclasses, Lobatto methods form an important family based on Gauss–Lobatto quadrature formulas and are characterized by the inclusion of both endpoints of the integration interval as collocation points. (Hairer, Nørsett & Wanner (1993); Iserles (2009); (Kahaner, 1989))

Let $y \in \mathbb{R}^d, f: \mathbb{R} \times \mathbb{R}^d \to \mathbb{R}^d,\ y' = f\big(x, y(x)\big),\ y(x_0) = y_0 \ for\ \ x \geq x_0$ (2.1)

initial value problem for a first-order ordinary differential equation. For the numerical solution of this initial value problem , some commonly utilized implicit Runge-Kutta methods are: Backward Euler Method, Implicit Midpoint Method, Crank-Nicolson Method, Gauss-Legendre Method, Diagonally Implicit

Runge-Kutta (DIRK) Methods, Lobatto IIIB Method, Lobatto IIIC Method, Lobatto IIIC* Method, Generalized Lobatto Method (Burden&Faires,2011).

The s-stage Runge-Kutta method $y_{n+1} \approx y(t_n + h)$ from $y_n \approx y(t_n)$ using the following formulas

$$k_i = y_n + h \sum_{j=1}^{s} a_{ij} f\left(t_n + c_j h, k_j\right), \quad (1 \leq i \leq s)$$

$$y_{n+1} = y_n + h \sum_{i=1}^{s} b_i f(t_n + c_i h, k_i)$$

where s, denotes the number of stages, a_{ij} represent the internal stage coefficients, b_i denote the weights, and c_i denote the abscissae (Butcher, 1964;Prince,Dormand,1981; Pareschi, Russo,2001; Iserles, 2009; Liu,Sun, 2005).

Figure 1: The Butcher tableau for the Runge-Kutta methods (Butcher, 1964)

$$\begin{array}{c|ccccc}
0 & & & & & \\
c_2 & a_{21} & & & & \\
c_3 & a_{31} & a_{32} & & & \\
\vdots & \vdots & & & & \\
c_s & a_{s1} & a_{s2} & \cdots & a_{ss-1} & \\
\hline
 & b_1 & b_2 & \cdots & b_{s-1} & b_s
\end{array}$$

The significance of these simplifying assumptions can be traced back to a result obtained by Butcher. The coefficients a_{ij}, c_j and b_j by which the s-stage Runge-Kutta methods are defined, are presented in the Butcher tableau as shown below.

$$\begin{array}{c|c} \mathbf{c} & \mathbf{A} \\ \hline & \mathbf{b}^{\mathrm{T}} \end{array} = \begin{array}{c|ccc}
c_1 & a_{11} & \cdots & a_{1s} \\
\vdots & \vdots & \ddots & \vdots \\
c_s & a_{s1} & \cdots & a_{ss} \\
\hline
 & b_1 & \cdots & b_s
\end{array}$$

Figure 2: The Butcher Tableau for s-stage Runge-Kutta method (Butcher, 1964;Liu & Sun,2005)

For consistency, the row-sum condition $c_i = \sum_{j=1}^{s} a_{ij}$ is usually imposed. If $a_{ij} = 0$ for all $j \geq i$, the method is explicit; otherwise it is implicit.

3. Lobatto Methods

Among the family of Runge-Kutta algorithms, Lobatto methods represent a particularly important subclass in the numerical treatment of differential equations. These schemes are also commonly known as Gauss-Lobatto formulas (Boscarino et al., 2015). A key feature of Lobatto methods is that the two ends of the interval serve as collocation points; this arrangement makes it possible to achieve high-order accuracy without sacrificing robust stability. This balance of accuracy and stability has made Lobatto methods widely used in engineering, physics, and applied mathematics. The literature recognizes several distinct subfamilies Lobatto IIIA, IIIB, IIIC, and IIIC*-each offering its own set of numerical characteristics, and all of them are classified as implicit Runge-Kutta methods.

Gauss–Lobatto formulas: The approximation employed for the solution of the problem (2.1) can be expressed by means of a standard quadrature formula in the form

$$\int_{t_n}^{t_n+h} f(t)dt \approx h_n\left(\sum_{i=1}^{s} b_i f(t_n + c_i h_n)\right).$$

where the step size is denoted by h_n , the weight coefficients by $b_1, \dots, b_s$ and the node coefficients by $c_1, \dots, c_s$.

Lobatto quadrature formulas (Gauss-Lobatto formulas) are defined for $s \geq 2$ by a construction that meets a prescribed set of node and weight conditions. The nodes c_i are taken as the roots of the polynomial

$$\frac{d^{s-2}}{dt^{s-2}}\left(t^{s-1}(1-t)^{s-1}\right).$$

and they are ordered so that the condition $c_1 = 0 < c_2 < \cdots < c_s = 1$ is satisfied. The weights and nodes together fulfill the requirement:

$$B(p): \sum_{i=1}^{s} b_i c_i^{k-1} = \frac{1}{k}, \qquad k = 1, \dots, p$$

Lobatto quadrature formulas possess a symmetric structure, i.e.,

$b_{s+1-j} = b_j, \quad c_{s+1-j} = 1 - c_j$ (Jay, 1996; Jay,2015).

3.1 The Lobatto Subfamilies

For a fixed number of stages s, nodes c_j and the weights b_j of the associated Lobatto quadrature formula are shared across the various Lobatto families. Consequently, these families are distinguished exclusively by their internal stage coefficients a_{ij}. While several equivalent definitions of these families exist in the literature, their coefficients a_{ij} can be explicitly specified through simplifying assumptions in a linearly implicit form:

$$C(q): \sum_{j=1}^{s} a_{ij} c_j^{k-1} = \frac{c_i^k}{k}$$

$$D(r): \sum_{i=1}^{s} b_i c_i^{k-1} a_{ij} = \frac{b_j}{k}\left(1 - c_j^k\right)$$

Lobatto IIIA:

The Lobatto IIIA method is a three-stage Lobatto method. By this method, the values of the function are estimated at three points within the interval, with the endpoints of the interval also being included. The Lobatto IIIA method is symmetric, and its order is $2s - 2$.

$$Y_{n2} = \frac{1}{2}(y_n + y_{n+1}) + \frac{h_n}{8}(f(t_n, y_n) - f(t_{n+1}, y_{n+1}))$$

$$y_{n+1} = y_n + \frac{h_n}{6}(f(t_n, y_n) + 4f(t_{n+1}, Y_{n2}) + f(t_{n+1}, y_{n+1}))$$

where $t_{n+1/2} = t_n + h_{n/2}$.

Figure 3: The Butcher Tableau for $s = 2,3,4,5$ (Jay,2015)

0	0	0
1	$\frac{1}{2}$	$\frac{1}{2}$
$A_{s=2}$	$\frac{1}{2}$	$\frac{1}{2}$

0	0	0	0
$\frac{1}{2}$	$\frac{5}{24}$	$\frac{1}{3}$	$-\frac{1}{24}$
1	$\frac{1}{6}$	$\frac{2}{3}$	$\frac{1}{6}$
$A_{s=3}$	$\frac{1}{6}$	$\frac{2}{3}$	$\frac{1}{6}$

0	0	0	0	0
$\frac{1}{2}-\frac{\sqrt{5}}{10}$	$\frac{11+\sqrt{5}}{120}$	$\frac{25-\sqrt{5}}{120}$	$\frac{25-13\sqrt{5}}{120}$	$\frac{-1+\sqrt{5}}{120}$
$\frac{1}{2}+\frac{\sqrt{5}}{10}$	$\frac{11-\sqrt{5}}{120}$	$\frac{25+13\sqrt{5}}{120}$	$\frac{25+\sqrt{5}}{120}$	$\frac{-1-\sqrt{5}}{120}$
1	$\frac{1}{12}$	$\frac{5}{12}$	$\frac{5}{12}$	$\frac{1}{12}$
$A_{s=4}$	$\frac{1}{12}$	$\frac{5}{12}$	$\frac{5}{12}$	$\frac{1}{12}$

0	0	0	0	0	0
$\frac{1}{2}-\frac{\sqrt{21}}{14}$	$\frac{119+3\sqrt{21}}{1960}$	$\frac{343-9\sqrt{21}}{2520}$	$\frac{392-96\sqrt{21}}{2205}$	$\frac{343-69\sqrt{21}}{2520}$	$\frac{-21+3\sqrt{21}}{1960}$
$\frac{1}{2}$	$\frac{13}{320}$	$\frac{392+105\sqrt{21}}{2880}$	$\frac{8}{45}$	$\frac{392-105\sqrt{21}}{2880}$	$\frac{3}{320}$
$\frac{1}{2}+\frac{\sqrt{21}}{14}$	$\frac{119-3\sqrt{21}}{1960}$	$\frac{343+69\sqrt{21}}{2520}$	$\frac{392+96\sqrt{21}}{2205}$	$\frac{343+9\sqrt{21}}{2520}$	$\frac{-21-3\sqrt{21}}{1960}$
1	$\frac{1}{20}$	$\frac{49}{180}$	$\frac{16}{45}$	$\frac{49}{180}$	$\frac{1}{20}$
$A_{s=5}$	$\frac{1}{20}$	$\frac{49}{180}$	$\frac{16}{45}$	$\frac{49}{180}$	$\frac{1}{20}$

Lobatto IIIB

The coefficients of the Lobatto IIIB, a_{ij}^B are defined through the simplifying assumption $D(r)$. These methods are required to satisfy the condition $C(q-2), a_{i1}^B = b_1, a_{is}^B = 0$. They are symmetric, and their order is $2s - 2$. The coefficients of the method can also be derived from the coefficients of Lobatto IIIA by means of the following relations:

$$a_{ij}^B b_i + a_{ji}^A b_j - b_j b_i = 0$$

or

$$a_{ij}^B = b_j - a_{s+1-i,s+1-j}^A$$

Figure 4: The Butcher Tableau for $s = 2,3,4,5$ (Jay,2015)

0	$\frac{1}{2}$	0
1	$\frac{1}{2}$	0
$B_{s=2}$	$\frac{1}{2}$	$\frac{1}{2}$

0	$\frac{1}{6}$	$-\frac{1}{6}$	0
$\frac{1}{2}$	$\frac{1}{6}$	$\frac{1}{3}$	0
1	$\frac{1}{6}$	$\frac{5}{6}$	0
$B_{s=3}$	$\frac{1}{6}$	$\frac{2}{3}$	$\frac{1}{6}$

0	$\frac{1}{12}$	$\frac{-1-\sqrt{5}}{24}$	$\frac{-1+\sqrt{5}}{24}$	0
$\frac{1}{2}-\frac{\sqrt{5}}{10}$	$\frac{1}{12}$	$\frac{25+\sqrt{5}}{120}$	$\frac{25-13\sqrt{5}}{120}$	0
$\frac{1}{2}+\frac{\sqrt{5}}{10}$	$\frac{1}{12}$	$\frac{25+13\sqrt{5}}{120}$	$\frac{25-\sqrt{5}}{120}$	0
1	$\frac{1}{12}$	$\frac{11-\sqrt{5}}{24}$	$\frac{11+\sqrt{5}}{24}$	0
$B_{s=4}$	$\frac{1}{12}$	$\frac{5}{12}$	$\frac{5}{12}$	$\frac{1}{12}$

0	$\frac{1}{20}$	$\frac{-7-\sqrt{21}}{120}$	$\frac{1}{15}$	$\frac{-7+\sqrt{21}}{120}$	0
$\frac{1}{2}-\frac{\sqrt{21}}{14}$	$\frac{1}{20}$	$\frac{343+9\sqrt{21}}{2520}$	$\frac{56-15\sqrt{21}}{315}$	$\frac{343-69\sqrt{21}}{2520}$	0
$\frac{1}{2}$	$\frac{1}{20}$	$\frac{49+12\sqrt{21}}{360}$	$\frac{8}{45}$	$\frac{49-12\sqrt{21}}{360}$	0
$\frac{1}{2}+\frac{\sqrt{21}}{14}$	$\frac{1}{20}$	$\frac{343+69\sqrt{21}}{2520}$	$\frac{56+15\sqrt{21}}{315}$	$\frac{343-9\sqrt{21}}{2520}$	0
1	$\frac{1}{20}$	$\frac{119-3\sqrt{21}}{360}$	$\frac{13}{45}$	$\frac{119+3\sqrt{21}}{360}$	0
$B_{s=5}$	$\frac{1}{20}$	$\frac{49}{180}$	$\frac{16}{45}$	$\frac{49}{180}$	$\frac{1}{20}$

Lobatto IIIC

The coefficients of the Lobatto IIIC satisfy the conditions

$$a_{i1}^C = b_1, \quad C(q-1), \qquad D(r-1), \quad a_{sj}^C = b_j$$

The order of this method is $2s - 2$. It is not symmetric. The formula for Lobatto IIIC methods is expressed as follows:

$$y_{n+1} = y_n + h\sum_{i=1}^{s} b_i k_i$$

$$k_i = f(t_n + c_i h, y_n + h\sum_{j=1}^{s} a_{ij} k_j)$$

Figure 5: The Butcher Tableau for $s = 2,3,4,5$ için Butcher tablosu (Jay,2015)

$$\begin{array}{c|cc} 0 & \frac{1}{2} & -\frac{1}{2} \\ 1 & \frac{1}{2} & \frac{1}{2} \\ \hline C_{s=2} & \frac{1}{2} & \frac{1}{2} \end{array} \qquad \begin{array}{c|ccc} 0 & \frac{1}{6} & -\frac{1}{3} & \frac{1}{6} \\ \frac{1}{2} & \frac{1}{6} & \frac{5}{12} & -\frac{1}{12} \\ 1 & \frac{1}{6} & \frac{2}{3} & \frac{1}{6} \\ \hline C_{s=3} & \frac{1}{6} & \frac{2}{3} & \frac{1}{6} \end{array} \qquad \begin{array}{c|cccc} 0 & \frac{1}{12} & -\frac{\sqrt{5}}{12} & \frac{\sqrt{5}}{12} & -\frac{1}{12} \\ \frac{1}{2}-\frac{\sqrt{5}}{10} & \frac{1}{12} & \frac{1}{4} & \frac{10-7\sqrt{5}}{60} & \frac{\sqrt{5}}{60} \\ \frac{1}{2}+\frac{\sqrt{5}}{10} & \frac{1}{12} & \frac{10+7\sqrt{5}}{60} & \frac{1}{4} & -\frac{\sqrt{5}}{60} \\ 1 & \frac{1}{12} & \frac{5}{12} & \frac{5}{12} & \frac{1}{12} \\ \hline C_{s=4} & \frac{1}{12} & \frac{5}{12} & \frac{5}{12} & \frac{1}{12} \end{array}$$

$$\begin{array}{c|ccccc} 0 & \frac{1}{20} & -\frac{7}{60} & \frac{2}{15} & -\frac{7}{60} & \frac{1}{20} \\ \frac{1}{2}-\frac{\sqrt{21}}{14} & \frac{1}{20} & \frac{29}{180} & \frac{47-15\sqrt{21}}{315} & \frac{203-30\sqrt{21}}{1260} & -\frac{3}{140} \\ \frac{1}{2} & \frac{1}{20} & \frac{329+105\sqrt{21}}{2880} & \frac{73}{360} & \frac{329-105\sqrt{21}}{2880} & \frac{3}{160} \\ \frac{1}{2}+\frac{\sqrt{21}}{14} & \frac{1}{20} & \frac{203+30\sqrt{21}}{1260} & \frac{47+15\sqrt{21}}{315} & \frac{29}{180} & -\frac{3}{140} \\ 1 & \frac{1}{20} & \frac{49}{180} & \frac{16}{45} & \frac{49}{180} & \frac{1}{20} \\ \hline C_{s=5} & \frac{1}{20} & \frac{49}{180} & \frac{16}{45} & \frac{49}{180} & \frac{1}{20} \end{array}$$

Lobatto IIIC*

The coefficients of the Lobatto IIIC* can be defined in the form a_{ij}^{C*}. The simplifying condition . $C(q-1)$ is satisfied by these methods. The order of this method is $2s-2$. It is not symmetric. The formula for the Lobatto IIIC* methods is expressed as follows:

$$a_{ij}^{C^*} b_i + a_{ji}^{C} b_j - b_j b_i = 0$$

or

$$a_{ij}^{C^*} = b_j - a_{s+1-i,s+1-j}^{C}, \quad i,j = 1,2,\dots,s$$

Figure 6: The Butcher Tableau for s = 2,3,4,5 için Butcher tablosu (Jay,2015)

$$\begin{array}{c|cc} 0 & 0 & 0 \\ 1 & 1 & 0 \\ \hline C^*_{s=2} & \frac{1}{2} & \frac{1}{2} \end{array} \qquad \begin{array}{c|ccc} 0 & 0 & 0 & 0 \\ \frac{1}{2} & \frac{1}{4} & \frac{1}{4} & 0 \\ 1 & 0 & 1 & 0 \\ \hline C^*_{s=3} & \frac{1}{6} & \frac{2}{3} & \frac{1}{6} \end{array} \qquad \begin{array}{c|cccc} 0 & 0 & 0 & 0 & 0 \\ \frac{1}{2}-\frac{\sqrt{5}}{10} & \frac{5+\sqrt{5}}{60} & \frac{1}{6} & \frac{15-7\sqrt{5}}{60} & 0 \\ \frac{1}{2}+\frac{\sqrt{5}}{10} & \frac{5-\sqrt{5}}{60} & \frac{15+7\sqrt{5}}{60} & \frac{1}{6} & 0 \\ 1 & \frac{1}{6} & \frac{5-\sqrt{5}}{12} & \frac{5+\sqrt{5}}{12} & 0 \\ \hline C^*_{s=4} & \frac{1}{12} & \frac{5}{12} & \frac{5}{12} & \frac{1}{12} \end{array}$$

$$\begin{array}{c|ccccc} 0 & 0 & 0 & 0 & 0 & 0 \\ \frac{1}{2}-\frac{\sqrt{21}}{14} & \frac{1}{14} & \frac{1}{9} & \frac{13-3\sqrt{21}}{63} & \frac{14-3\sqrt{21}}{126} & 0 \\ \frac{1}{2} & \frac{1}{32} & \frac{91+21\sqrt{21}}{576} & \frac{11}{72} & \frac{91-21\sqrt{21}}{576} & 0 \\ \frac{1}{2}+\frac{\sqrt{21}}{14} & \frac{1}{14} & \frac{14+3\sqrt{21}}{126} & \frac{13+3\sqrt{21}}{63} & \frac{1}{9} & 0 \\ 1 & 0 & \frac{7}{18} & \frac{2}{9} & \frac{7}{18} & 0 \\ \hline C^*_{s=5} & \frac{1}{20} & \frac{49}{180} & \frac{16}{45} & \frac{49}{180} & \frac{1}{20} \end{array}$$

Generalized Lobatto:

Generalized Lobatto methods constitute a consistent and efficient class of methods that can be applied to numerical solution problems. The formula of the generalized Lobatto methods is expressed as follows:

$$a_{ij}^{s}\left(\frac{1}{2}\right) = \frac{1}{2}\left(a_{ij}^{A} + a_{ij}^{B}\right) \qquad i,j = 1,\dots,s$$

For particular parameter selections, generalized Lobatto methods reduce to well-known classical Lobatto schemes such as Lobatto IIID

$$a_{ij}^{D} = a_{ij}^{S}(1) = \frac{1}{2}\left(a_{ij}^{C} + a_{ij}^{C^*}\right) \quad i,j = 1,\dots,s$$

Figure 7: The coefficients of Lobatto III-NW for s = 2, 3 (Butcher, 1964)

$$\begin{array}{c|cc} 0 & \frac{1}{2} & \frac{1}{2} \\ 1 & -\frac{1}{2} & \frac{1}{2} \\ \hline & \frac{1}{2} & \frac{1}{2} \end{array} \qquad \begin{array}{c|ccc} 0 & \frac{1}{6} & 0 & -\frac{1}{6} \\ \frac{1}{2} & \frac{1}{12} & \frac{5}{12} & 0 \\ 1 & \frac{1}{2} & \frac{1}{3} & \frac{1}{6} \\ \hline & \frac{1}{6} & \frac{2}{3} & \frac{1}{6} \end{array}$$

3.2 Stability properties

Lobatto methods belong to the class of high-order implicit Runge-Kutta methods, and among their most critical attributes is stability. To investigate the stability properties of a Runge–Kutta method, the Dahlquist test equation is conventionally employed:

$$y' = \lambda y$$

where $\lambda \in \mathbb{C}$ and the quantity $z = h\lambda$ is introduced. For a general *s*-stage Runge-Kutta method, the stability function takes the form

$$R(z) = zb^{T}(I - zA)^{-1}e{+}1$$

in which *A* denotes the coefficient matrix of the method, *b* is the weight vector, and $e = (1,\dots,1)^{T}$ is the vector.

Definition 3.2.1 (Absolute Stability) The stability region of a numerical method is defined as the set

$$S = \{z \in \mathbb{C} : |R(z)| \leq 1\}$$

For all values of z that lie within this region, the growth of the numerical solution is prevented, and stable behavior of the method is ensured (Lambert, 1991).

Definition 3.2.2 (A-Stability) A numerical method is called A-stable if its region of absolute stability contains the entire left half of the complex plane, i.e. if the set inclusion

$$\{z \in \mathbb{C} : Re(z) \leq 0\} \subseteq S$$

is satisfied. Equivalently, the stability function must satisfy

$$|R(z)| \leq 1. \qquad Re(z) \leq 0$$

(Hairer, Nørsett, and Wanner, 1993).

Definition 3.2.3 (L-Stability). A method is called L-stable if it is A-stable and, in addition, the condition

$$\lim_{z \to -\infty} R(z) = 0$$

is satisfied (Hairer, Wanner,,1996).

Definition 3.2.4 (B-stability) A numerical method is called B-stable if, for any system for which the inner-product condition

$$\langle f(u) - f(v), u - v \rangle \leq 0$$

is satisfied, the contractivity property

$$||y_{n+1} - \widetilde{y_{n+1}}|| \leq ||y_n - \widetilde{y_n}||$$

holds for any two numerical solutions $\{y_n\}$ and $\{\widetilde{y_n}\}$. In other words, it may be expressed equivalently as the condition that the separation between any two numerical solution trajectories is non-increasing throughout the integration interval. (Butcher, 2016).

Definition 3.2.5 (Algebraic stability) In the context of a Runge–Kutta method, let the weights satisfy $b_i \geq 0 \quad (i = 1,2,..,s)$ and let the matrix $M = (m_{ij})$ be defined by

$$m_{ij} = a_{ij}b_i + a_{ji}b_j - b_j b_i.$$

If M is positive semi-definite ($M \geq 0$), the method is called to be algebraically stable (Hairer and Wanner, 1996).

Definition 3.2.6 (AN-stability) A method is called AN-stable if its stability region, while not necessarily covering the entire left half-plane, contains the sector

$$\{z : |\arg(-z)| \leq \alpha\}$$

for some angle $0 < \alpha < 90^o$. In the special case $\alpha = 90^o$, A-stability is recovered (Butcher, 2016).

Definition 3.2.7 (G-stability) A numerical method is called G-stable if there exists a symmetric positive-definite matrix $G = G^T > 0$ such that, in the G-norm $\|y\|_G = \sqrt{y^T G y}$, the inequality

$$\|y_{n+1}\|_G \leq \|y_n\|_G$$

holds for all numerical solutions (Dahlquist, 1978).

Definition 3.2.8 (Zero-stability). Let the characteristic polynomial be denoted by $\rho(r)$ and suppose that $\rho(r) = 0$. A method is zero-stable if all roots r_i satisfy $|r_i| \leq 1$ and any root for which $|r_i| = 1$ is simple (Lambert,1991).

Definition 3.2.9 (P-stability) A method is called P-stable if, when applied to the oscillator equation $y'' + \omega 2y = 0y'' + \omega 2y = 0$, no artificial numerical damping occurs, i.e., $|\ R(iy)\ | = 1$ for all real y (Hairer & Wanner, 1996).

Definition3.2.10 (Padé Approximation) The Padé approximant of order (p, q) to the exponential function $e^{\ z}$ is the unique rational function

$$R_{p,q}(z) = \frac{N_{p,q}(z)}{D_{p,q}(z)} = \frac{\sum_{k=0}^{p} z^k \alpha_k}{\sum_{k=0}^{q} z^k \beta_k}$$

where $\beta_0 = 1$, such that, satisfying the interpolation condition

$$e^z - R_{p,q}(z) = O(zp + q + 1), \ \ z \to 0.$$

The coefficients are given explicitly by

$$\alpha_k = \frac{(p+q-k)!p!}{(p+q)!k!(p-k)!}, \quad \beta_k = \frac{(p+q-k)!q!}{(p+q)!k!(q-k)!}$$

(Hairer & Wanner, 1996).

Definition3.2.11 (Absolute Stability Boundary) For a given Lobatto method, the absolute stability boundary is defined by the relation $|R(z)| = 1$. The stability region is the set of all points satisfying the condition $|R(z)| \leq 1$. For instance, in the case of the three-stage Lobatto IIIA, IIIB, and IIIC, generalized Lobatto and LobattoIIID methods, the stability function is given by

$$R_{IIIA}(z) = R_{IIIB}(z) = \frac{\frac{1}{12}z^2 + \frac{1}{2}z + 1}{\frac{1}{12}z^2 - \frac{1}{2}z + 1},$$

$$R_{IIIC}(z) = \frac{\frac{1}{2}z + 1}{\frac{1}{6}z^2 - \frac{1}{2}z + 1}$$

$$R_{IIIC^*}(z) = \frac{1}{R_{IIIC}(-z)} = \frac{\frac{1}{6}z^2 + \frac{1}{2}z + 1}{-\frac{1}{2}z + 1}$$

$$R_{GL}(z) = R_{IIID}(z) = \frac{\frac{1}{12}z^2 + \frac{1}{2}z + 1}{\frac{1}{12}z^2 - \frac{1}{2}z + 1}$$

(Dahlquist, 1978; Hairer,, Wanner, 1996; Butcher, 2016).

For the three-stage case, Lobatto IIIA, IIIB and IIID share the same stability function, whereas Lobatto IIIC possesses a distinct stability function associated with its stiffly accurate structure. Generalized Lobatto methods do not admit a unique stability function, since their properties depend on the specific parameter selection.

Table 1. Comparison of Stability and Geometric Properties of Lobatto Families

Property	**IIIA**	**IIIB**	**IIIC**	**IIIC***	**IIID**	**Generalized Lobatto**	
Implicit Method	Yes	Yes	Yes	Yes	Yes	Yes	16,17,23,27,32
Symmetric	Yes	Yes	No	No	No	Parameter-dependent	17,24,25,28
Order (s-stage)	2s−2	2s−2	2s−2	2s−2	2s−2	Depends on construction	15,17,24,28,32
A-Stable	Yes	Yes	Yes	Yes	Yes	Usually Yes	16,17,19,20,23,24
L-Stable	No	No	Yes	No	No	Parameter-dependent	17,20,24,32
AN-Stable	Yes	Yes	Yes	Yes	Yes	Usually Yes	6,17,24
Zero-Stable	Yes	Yes	Yes	Yes	Yes	Yes	11,17,23,31
B-Stable	No	No	Yes	No	Generally no	Parameter-dependent	17,20,24
Algebraically Stable	No	No	Yes	No	Generally no	Parameter-dependent	17,20,24
G-Stable	Yes	Yes	Yes	Generally No	Yes	Parameter-dependent	17,18,23,24
P-Stable	Generally no	Generally no	Generally no	Generally no	Generally no	Usually No	6,17,24
Stiffly Accurate	No	No	Yes	No	Yes	Parameter-dependent	17,20,24,32
Symplectic (single method)	No	No	No	No	No	Parameter-dependent	17,23,25
Symplectic Pair	IIIA–IIIB	IIIA–IIIB	None	None	None	Possible	17,23,25,28
Energy Behavior	Good	Good	Strong damping	Dissipative	Good damping	Parameter-dependent	17,23,24,25
Imaginary-Axis Behavior	Nearly conservative	Nearly conservative	Damped	Damped	Moderately damped	Parameter-dependent	17,18,24,25
High-Frequency Damping	Weak	Weak	Strong	Moderate	Strong	Parameter-dependent	17,20,23,24
Suitable for Stiff ODEs	Moderate	Moderate	Excellent	Moderate	Excellent	Depends on parameters	17,20,24,32
Suitable for DAEs	Good	Moderate	Excellent	Moderate	Excellent	Depends on formulation	17,20,24,32
Suitable for Hamiltonian Systems	Via IIIA–IIIB pair	Via IIIA–IIIB pair	Limited	Limited	Limited	Possible	17,23,25,28
Boundary Value Problems	Excellent	Good	Excellent	Good	Excellent	Excellent	1,17,23,24
Typical Applications	Collocation methods	Partitioned systems	Stiff systems and DAEs	Specialized IRK methods	DAEs and stiff problems	Problem-dependent	6,17,23,24, 25,28,29,32

3.3 Lobatto Families and Absolute Stability Regions

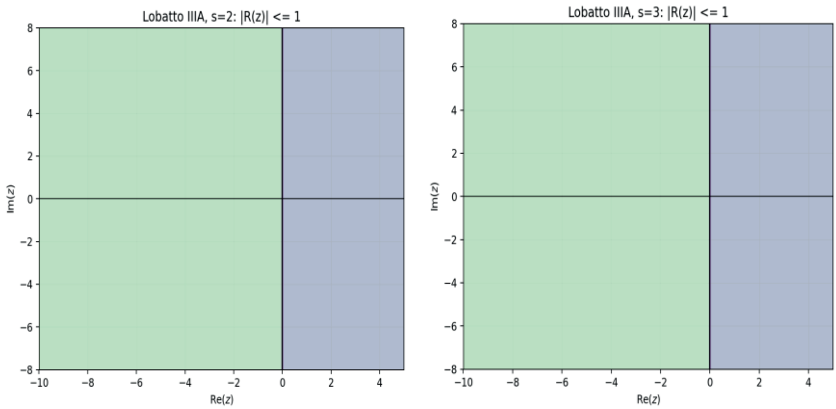

Figure 8: Absolute stability regions for Lobatto IIIA method for s=2 (left) and s=3 (right)

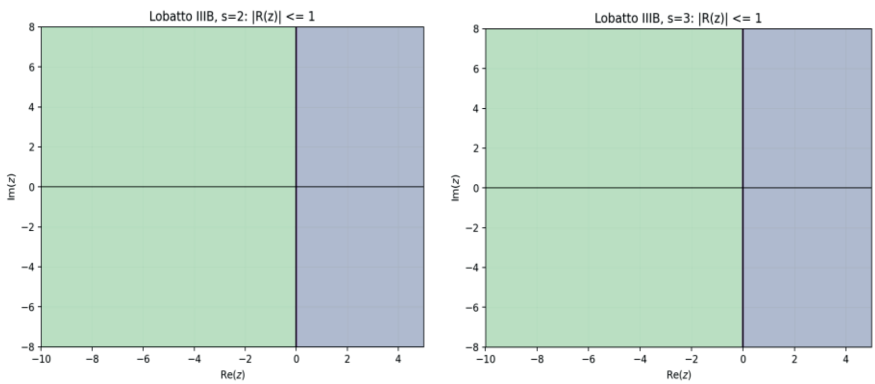

Figure 9: Absolute stability regions for Lobatto IIIB method for s=2 (left) and s=3 (right)

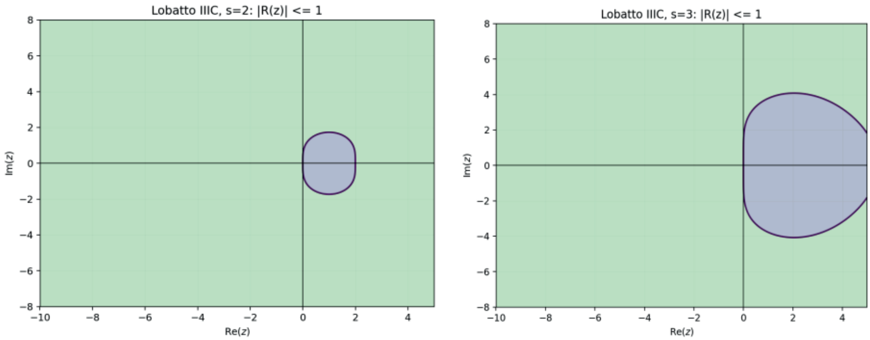

Figure 10: Absolute stability regions for Lobatto IIIC method for s=2 (left) and s=3 (right)

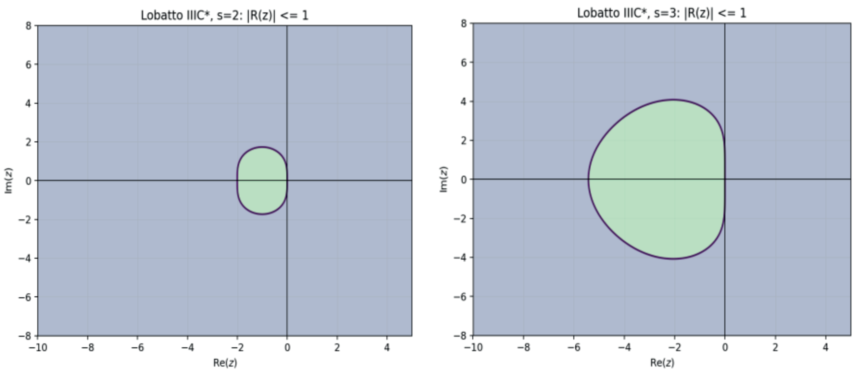

Figure 11: Absolute stability regions for Lobatto IIIC* methods with s=2 (left) and s=3 (right)

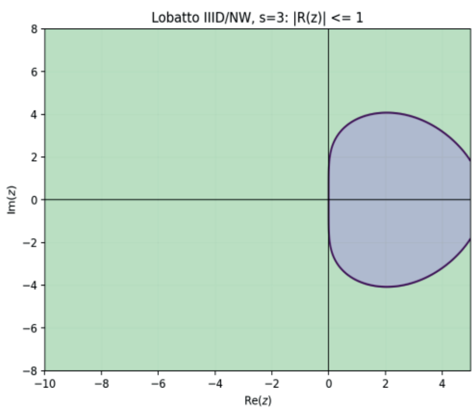

Figure 12: Absolute stability regions for Lobatto IIID/Nørsett-Wanner method for s=3

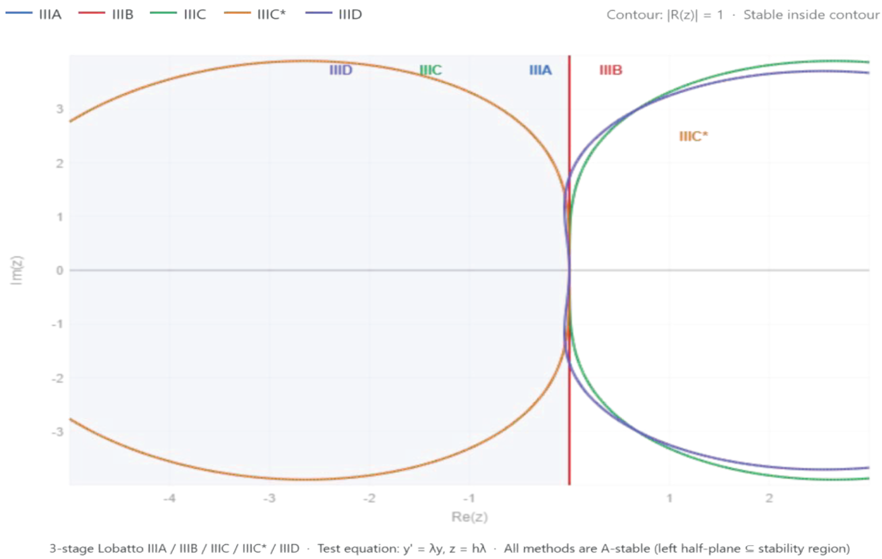

Figure 13: Absolute stability regions of the 3-stage Lobatto IIIA, IIIB, IIIC, IIIC*, and IIID methods

All figures were generated using the Maple software package. As observed in Figure $8 - 13$, the shaded regions show where $|R(z)| \leq 1$ in the absolute stability plots. Since . $z = h\lambda$ is defined, the point is shifted to the left as either the step size h is increased or λ becomes more negative. Because large negative real values are of primary concern in stiff problems, the behavior within the left half-plane is considered the deciding factor.

In the plots for the Lobatto IIIA and IIIB methods, the left half-plane is fully contained within the stability region; thus, A-stability is implied. However, it is noted that as $|z| \to \infty$ along the negative real axis, $R(z)$ is not driven to zero. Consequently, very stiff modes are not completely suppressed. In the diagrams, this is evidenced by the fact that the method's stability function is shown to approach a magnitude of 1 at infinity, even though the negative real axis remains within the stable region.

In the case of Lobatto IIIC and IIID/NW plots, the behavior $R(z) \to 0$ is observed along the negative real axis. Through this property, stiff modes are suppressed more effectively by these methods. This feature is particularly advantageous for parabolic-type or strongly dissipative systems, allowing more reliable integration with large step sizes.

4. Conclusion

Ordinary differential equations (ODEs) provide a fundamental framework for modeling dynamical systems across a multitude of scientific and engineering disciplines Since analytical solutions are rarely available for such systems, robust numerical methods have become essential in computational mathematics. These methods approximate the solution at discrete nodes over a given interval. The goal is to capture the continuous behavior of the system as accurately as possible. Among the most prevalent numerical frameworks utilized to achieve this are the Runge-Kutta (RK) algorithms. While explicit RK schemes offer computational efficiency for non-stiff problems, the presence of stiff systems stiff systems, characterized by widely separated time scales, require implicit methods mandates the deployment of implicit methods to ensure stability without the computational burden of prohibitively small step sizes. Within the broader class of implicit Runge-Kutta (IRK) schemes, collocation-based methods are distinguished by high-order accuracy coupled with a continuous representation of the analytical solution. Grounded in Gauss-Lobatto quadrature, the Lobatto family occupies a particularly prominent position within this collocation framework. The distinct mathematical signature of Lobatto methods is the explicit requirement that the interpolating polynomial strictly satisfies the differential equation at both the initial and final boundaries of the integration step, formally defined by setting the collocation nodes to $c_1 = 0$ and $c_s = 1$. Because of this deliberate endpoint inclusion, some members of the Lobatto family possess additional properties such as stiff accuracy and enhanced continuity and global continuity, which is particularly useful for boundary value problems and optimal control. Consequently, the distinct subfamilies, namely Lobatto IIIA, IIIB, IIIC, and IIIC*, exhibit a rich spectrum of stability profiles, ranging from the purely A-stable and good geometric properties of the IIIA class to the rigorously L-stable and strongly damped behavior of the IIIC variant.

References

1. Ascher, U. M., Ruuth, S. J., & Wetton, B. T. (1995). Implicit-explicit methods for time-dependent partial differential equations. SIAM Journal on Numerical Analysis, 32(3), 797-823.
2. Atkinson, E., Han, W. ve Stewart, D. (2008). Numerical Solution of Ordinary Differential Equations, 2.Baskı, John Wiley&Sons, New Jersey.
3. Atkinson, K.E., Han W and Stewart D.E., 2009, Numerical Solution of Ordinary Differential Equations, Towa City, IA, 95-109.
4. Boscarino, S. 2007. Error analysis of IMEX Runge-Kutta methods derived from differential-algebraic systems. SIAM Journal on Numerical Analysis, 45(4), 1600-1621.
5. Boscarino, S. 2009. On an accurate third order implicit-explicit Runge-Kutta method for stiff problems. Applied Numerical Mathematics, 59(7), 1515-1528.
6. Boscarino, S., Bürger, R., Mulet, P., Russo, G., & Villada, L. M. 2015. Linearly implicit IMEX Runge-Kutta methods for a class of degenerate convection-diffusion problems. SIAM Journal on Scientific Computing, 37(2), B305-B331.
7. Brugnano, L., & Magherini, C. (2007). Blended implicit methods for solving ODE and DAE problems, and their extension for second-order problems. Journal of computational and applied mathematics, 205(2), 777-790.
8. Brugnano, L., Iavernaro, F., & Trigiante, D. 2012. Energy- and quadratic invariants–preserving integrators based upon Gauss collocation formulae. SIAM Journal on Numerical Analysis, 50(6), 2897–2916.
9. Brugnano, L., & Sun, Y. 2014. Multiple invariants conserving Runge-Kutta type methods for Hamiltonian problems. Numerical Algorithms, 65(3), 611–632.
10. Bulirsch, R., & Stoer, J. 2000. Introduction to numerical analysis. Springer-Verlag.
11. Burden, R.L., Fairs, J.D. 2010. Numerical Analysis. 9th Edition, Boston, MA: Brooks/Cole, Cengage Learning.
12. Burden, R. L., & Faires, J. D. (2011). Numerical differentiation & integration numerical differentiation I. Numerical analysis, 174-184.
13. Burrage, K. (1978a). Stability and efficiency properties of implicit Runge-Kutta methods. Bulletin of the Australian Mathematical Society, 19(2), 297-298.
14. Burrage, K. (1978b). A special family of Runge-Kutta methods for solving stiff differential equations. BIT Numerical Mathematics, 18(1), 22-41.
15. Butcher, J. C. 1987. The numerical analysis of ordinary differential equations I: Runge-Kutta and general linear methods. John Wiley & Sons.

16. Butcher, J. C. 1964. On Runge-Kutta processes of higher order, Journal of the Australian Mathematical Society, 4(2), 179-197.
17. Butcher, J.C., 2016. Numerical Methods for Ordinary Differential Equations, 3rd ed., John Wiley and Sons, Chichester.
18. Dahlquist, G. (1978). G-stability is equivalent to A-stability. BIT Numerical Mathematics, 18(4), 384-401.
19. Ehle, B. L. (1973). A-stable methods and Padé approximations to the exponential. SIAM Journal on Mathematical Analysis, 4(4), 671-680.
20. Frank, R., Schneid, J., & Ueberhuber, C. W. (1985). Stability properties of implicit Runge– Kutta methods. SIAM journal on numerical analysis, 22(3), 497-514.
21. Griepentrog, E., 1978, Gemischte Runge-Kutta-Verfahren für steife Systeme (Mixed Runge-Kutta Methods for Stiff Systems), Seminarberichte, vol. 11, Sektion Mathematik, Humboldt Universität, Berlin, pp. 19–29, in German.
22. Hairer, E., Lubich, C., & Roche, M. (1989). Error of Rosenbrock methods for stiff problems studied via differential algebraic equations. BIT Numerical Mathematics, 29(1), 77-90.
23. Hairer, E. Nørsett, S.P. Wanner, G. 1993. Solving Ordinary Differential Equations, I: Nonstiff Problems, 2 ed., Springer-Verlag, Berlin.
24. Hairer, E., & Wanner, G. 1996. Solving ordinary differential equations. II (2nd ed.). Springer Series in Computational Mathematics, 14. Berlin: Springer-Verlag.
25. Hairer, E., Lubich, C., & Wanner, G. 2006. Geometric numerical integration (2nd ed.). Springer Series in Computational Mathematics, 31. Berlin: Springer-Verlag.
26. Hairer, E., Wanner, G., & Nørsett, S. P. (1993). Solving ordinary differential equations I: Nonstiff problems. Berlin, Heidelberg: Springer Berlin Heidelberg.
27. Iserles, A. (2009). A first course in the numerical analysis of differential equations (No. 44). Cambridge university press.
28. Jay, L. O. (1996). Lobatto methods. chemistry, 29, 298-305.
29. Jay, L. O. (2015). Lobatto methods. Department of Mathematics, The University of Lowa, Lowa City, USA.
30. Kahaner, D., Moler, C., & Nash, S. (1989). Numerical methods and software. Prentice-Hall, Inc..
31. Lambert, J.D. (1991) Numerical Methods for Ordinary Differential Systems: The Initial Value Problem. John Wiley & Sons, Inc., Hoboken, Chapter 2, 21-44.
32. Liu, H., & Sun, G. (2005). Implicit Runge–Kutta methods based on Lobatto quadrature formula. International Journal of Computer Mathematics, 82(1), 77-88.

33. Martín-Vaquero, J. (2010). A 17th-order Radau IIA method for package RADAU. Applications in mechanical systems. Computers & Mathematics with Applications, 59(8), 2464-2472.
34. Pareschi, L., & Russo, G. 2001. Implicit-explicit Runge-Kutta schemes for stiff systems of differential equations. In Recent Trends in Numerical Analysis (Adv. Theory Comput. Math., vol. 3, pp. 269–288).
35. Prince, P.J. Dormand, J.R. 1981. High order embedded Runge–Kutta formulae, J. Comput. Appl. Math. 7 (1) 67–75.
36. Ranocha, H., Sayyari, M., Dalcin, L., Parsani, M., & Ketcheson, D. I. 2020. Relaxation Runge-Kutta methods: fully discrete explicit entropy-stable schemes for the compressible Euler and Navier-Stokes equations. SIAM Journal on Scientific Computing, 42(2), A612–A638.
37. Süli, E., & Mayers, D. F. (2003). An introduction to numerical analysis. Cambridge university press.